

Journal Pre-proofs

Genome-wide analyses reveals a glucosyltransferase involved in rutin and emodin glucoside biosynthesis in tartary buckwheat

Qinggong Yin, Xiaoyan Han, Zongxian Han, Qingfu Chen, Yuhua Shi, Han Gao, Tianyuan Zhang, Gangqiang Dong, Chao Xiong, Chi Song, Wei Sun, Shilin Chen

PII: S0308-8146(20)30340-X
DOI: <https://doi.org/10.1016/j.foodchem.2020.126478>
Reference: FOCH 126478

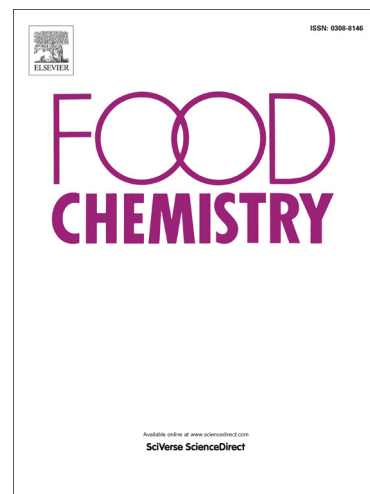
To appear in: *Food Chemistry*

Received Date: 3 October 2019
Revised Date: 23 February 2020
Accepted Date: 23 February 2020

Please cite this article as: Yin, Q., Han, X., Han, Z., Chen, Q., Shi, Y., Gao, H., Zhang, T., Dong, G., Xiong, C., Song, C., Sun, W., Chen, S., Genome-wide analyses reveals a glucosyltransferase involved in rutin and emodin glucoside biosynthesis in tartary buckwheat, *Food Chemistry* (2020), doi: <https://doi.org/10.1016/j.foodchem.2020.126478>

This is a PDF file of an article that has undergone enhancements after acceptance, such as the addition of a cover page and metadata, and formatting for readability, but it is not yet the definitive version of record. This version will undergo additional copyediting, typesetting and review before it is published in its final form, but we are providing this version to give early visibility of the article. Please note that, during the production process, errors may be discovered which could affect the content, and all legal disclaimers that apply to the journal pertain.

© 2020 Published by Elsevier Ltd.



1 **Genome-wide analyses reveals a glucosyltransferase involved in rutin and emodin glucoside**
2 **biosynthesis in tartary buckwheat**

3
4 Qinggang Yin^{1*} Xiaoyan Han^{2*} Zongxian Han³ Qingfu Chen⁴ Yuhua Shi¹ Han Gao³
5 Tianyuan Zhang¹ Gangqiang Dong⁵ Chao Xiong¹ Chi Song¹ Wei Sun^{1#} Shilin
6 Chen^{1#}

7
8 1. Key Laboratory of Beijing for Identification and Safety Evaluation of Chinese Medicine, Institute
9 of Chinese Materia Medica, China Academy of Chinese Medical Sciences, Beijing 100700,
10 China

11 2. Beijing Botanical Garden, Institute of Botany, Chinese Academy of Sciences, Beijing 100093,
12 China

13 3. School of Chemistry Chemical Engineering and Life Sciences, Wuhan University of Technology,
14 No. 122, Lo lion Road, Wuhan, Hubei, 430070, China

15 4. Research Center of Buckwheat Industry Technology, Guizhou Normal University, Baoshan Beilu
16 116, Guiyang 550001, China

17 5. Amway (China) Botanical R&D centre, Wuxi 214115, China

18 *These authors contributed equally to this work.

19 #Corresponding authors: Wei Sun, E-mail: wsun@icmm.ac.cn; Shilin Chen, E-mail:.

20 slchen@icmm.ac.cn, phone: 0086-01064014411.

21
22 **Highlights**

23 Temporal and spatial transcripts of 106 FtUGTs were analyzed in genome level.

24
25 FtUGT73BE5 was identified dominating the first step of rutin glycosylation.

26

27 FtUGT73BE5 was demonstrated to catalyze emodin to form emodin 6-*O*-glucoside.

28

29 MeJA up-regulates transcript of *FtUGT73BE5*; it was related to anti-adversity.

30

31 **Abstract**

32

33 With people's increasing needs for health concern, rutin and emodin in tartary buckwheat have
34 attracted much attention for their antioxidant, anti-diabetic and reducing weight function. However,
35 the biosynthesis of rutin and emodin in tartary buckwheat is still unclear; especially their later
36 glycosylation contributing to make them more stable and soluble is uncovered. Based on tartary
37 buckwheat' genome, the gene structures of 106 UGTs were analyzed; 21 candidate FtUGTs were
38 selected to enzymatic test by comparing their transcript patterns. Among them, FtUGT73BE5 and
39 other 4 FtUGTs were identified to glucosylate flavonol or emodin *in vitro*; especially
40 rFtUGT73BE5 could catalyze the glucosylation of all tested flavonoids and emodin. Furthermore,
41 the identical *in vivo* functions of FtUGT73BE5 were demonstrated in tartary buckwheat hairy roots.
42 The transcript profile of *FtUGT73BE5* was consistent with the accumulation trend of rutin in plant;
43 This gene may relate to anti-adversity for its transcripts were up-regulated by MeJA, and repressed
44 by ABA.

45

46 **Key words**

47

48 Tartary buckwheat; Rutin; Emodin; Glucoside; Biosynthesis; Glucosyltransferase; Genome-wide

49 **1 Introduction**

50

51 Tartary buckwheat (*Fagopyrum tataricum*) belongs to the genus *Fagopyrum*, a member of the
52 eudicot family Polygonaceae which comprises of about 23 species (Chen, 2018). Distributed in
53 subtropical and temperate regions, tartary buckwheat is planted especially in mountainous areas
54 where other crops such as rice and wheat are not adapted (Tsuji & Ohnishi, 2000; Liu, Chen, Yang,
55 & Chiang, 2008). Due to the beneficial values of flavonoids and emodin, tartary buckwheat is more
56 popular as a healthy food than a crop. Tartary buckwheat is an important natural source of
57 flavonoids for human, such as rutin, which are minor in main crops like rice (*Oryza sativa*), wheat
58 (*Triticum aestivum*), sorghum (*Sorghum bicolor*), highland barley (*Hordeum vulgare*) and soybean
59 (*Glycine max*) (Fabjan, Rode, Kosir, Wang, Zhang, & Kreft, 2003). Previous studies indicated that
60 these flavonoids have antioxidant, anti-diabetic, anti-inflammatory, anti-neuroprotective and
61 cytotoxic effects (Yasui *et al.*, 2016; Zhang *et al.*, 2017; Al-Snafi, 2017). Another functional
62 compound—emodin exists in tartary buckwheat, which plays a major role in preventing type II
63 diabetes and reducing weight according to recent reports (Lee, Ku, & Bae, 2013; Peng *et al.*, 2013).

64
65 Though the structures of rutin and emodin are different, they possess a common precursor malonyl
66 Co-A, catalyzed by polyketone synthase (PKS), and then stably exists in plant through the same
67 glycosylation (Fig.S1). Unmodified rutin is quercetin, which are biosynthesized by chalcone
68 synthase (CHS) which is a kind of PKS, chalcone isomerase (CHI), flavanone 3-hydroxylase (F3H),
69 flavanone 3'-hydroxylase (F3'H) and flavonol synthase (FLS) according to the study of model
70 plants, such as *Glycine max* (Rodas *et al.*, 2014) and *Citrus* (Frydman *et al.*, 2004). However, there
71 are few reports regarding to these genes in tartary buckwheat. The synthesis of emodin sorted to
72 anthraquinone is mainly through polyketone pathway (Bringmann & Irmer, 2008). The polyketone
73 pathway can be divided into 3 stages: octaketide chain were formed using acetyl Co-A and malonyl
74 Co-A as the starting substrates by PKS. After reduction, decarboxylation and oxidation,
75 chrysophanol, aloe emodin and rhein were formed from octaketide chain. Alternatively, emodin

76 could be produced by hydrolyzed, decarboxylation and dehydration of octaketide chain. Generally,
77 quercetin and emodin are finally modified by UDP-glycosyltransferase (UGT) to produce rutin and
78 emodin glycosides respectively.

79
80 Glycosides are the final form of rutin and emodin in plant, which determine their pharmaceutical
81 functions (Jing, Li, Hu, Jiang, Qin, & Zheng, 2014; Lee *et al.*, 2013). Glycosylation of rutin is
82 divided into two steps. First, quercetin is glucosylated by 3-hydroxyl, followed by rhamosylation of
83 the 6-hydroxyl of glucose group in quercetin 3-*O*-glucoside (An, Yang, Kim, & Ahn, 2016). FaGT6
84 (*Fragaria ananassa*), Cp3OGT (*Citrus paradisi*), GmUGT78K1 (*G. max*) and VvGT5 (*Vitis*
85 *Vinifera*) were *in vitro* proved to involve in the first step (Griesser *et al.*, 2008; Owens, & McIntosh,
86 2009; Kovinich, Saleem, Arnason, & Miki, 2010; Mizohata *et al.*, 2013), but their functions *in vivo*
87 are still blurry. GmUGT79A6, Cm1, 6RhaT and FeUGT79A8 (*F. esculentum*) were demonstrated
88 responsible for the second step of rutin glycosylation (Frydman *et al.*, 2004; Rodas *et al.*, 2014;
89 Koja, Ohata, Maruyama, Suzuki, Shimosaka, & Taguchi, 2018). A previous report identified three
90 UGTs involved in the glucosylation of cyanidin 3-*O*-glucoside in *F. tataricum* by enzymatic tests *in*
91 *vitro* (Zhou *et al.*, 2016), meanwhile FeCGTa (UGT708C1) and FeCGTb (UGT708C2) were
92 identified to have *C*-glucosylation activity toward 2-hydroxyflavanones, dihydrochalcone,
93 trihydroxyacetophenones and other related compounds with chemical structures similar to
94 2',4',6'-trihydroxyacetophenone (Nagatomo, Usui, Ito, Kato, Shimosaka, & Taguchi, 2014). Since
95 emodin possess very low solubility, the practical potency as oral medicine will be discounted
96 compared with its theoretical biological activity (Lee *et al.*, 2013). That was in accordance with
97 later report that the anthraquinone glucosides had higher bioavailability and better pharmacological
98 activity (Ghimire, Koirala, Pandey, Jung, & Sohng, 2015). Emodin exists 3 hydroxyls distributed 1-,
99 6- and 8- position, which would be the target of glycosylation. There is only one report about the
100 glucosylation of emodin in plant: CtUGT73AE1 catalyzed the formation of emodin 8-*O*-glucoside
101 *in vitro* (Xie *et al.*, 2014). However, no reports about glycosylation other positions of emodin has

102 been published to date. Usually the structure of protein determines its function in plants; it's
103 reasonable to speculate the homolog gene of *CtUGT73AE1* in tartary buckwheat may encode
104 similar functional protein.

105

106 The entire sequences from genome contribute to the feasibility for illuminating the superfamily of
107 protein, such as UGTs, which possess functional redundancy and diversity (Zhang *et al.*, 2017).
108 Based on the published genomes, integrated UGTs for their key secondary metabolites were
109 identified systematically, such as flavonoids in *Arabidopsis* and *L. japonicus*, 2-phenylethanol in
110 peach, andrographolide in *Andrographis paniculata* and ginsenoside in ginseng (Caputi, Malnoy,
111 Goremykin, Nikiforova, & Martens, 2012; Yin, Shen, Chang, Tang, Gao, & Pang, 2017; Wu *et al.*
112 2017; Xu *et al.* 2017; Sun *et al.* 2018). Equally predictable, the available genome of *F. tataricum*
113 would provide a scheme for the systematic analysis of the whole pathway of rutin synthesis,
114 especially for the analysis of UGTs.

115

116 Herein, using the available genome and transcriptome data of *F. tataricum*, we identified 106 UGT
117 genes. Among 14 cloned FtUGTs, not only FtUGT73BE5 was able to glycosylate all tested
118 flavonoids, but also could catalyze emodin to form emodin 6-*O*-glucoside *in vitro*. Subsequently,
119 the functions of FtUGT73BE5 were verified using *F. tataricum* hairy root system. Furthermore,
120 methyl-jasmonate (MeJA) were demonstrated to up-regulate the transcription of *FtUGT73BE5* and
121 slightly increase rutin content in seedlings. Our study sheds light on the functional diversity and
122 biochemical mechanism of UGTs, involving in the biosynthesis of rutin and emodin glucosides in *F.*
123 *tataricum*; these understandings would also benefit to developing healthy tartary buckwheat food.

124

125 2 Materials and Methods

126

127 2.1 Materials and chemicals

128

129 *F. tataricum* (BT18) plants were grown in an illumination incubator under control (16 h/8 h
130 day/night cycle at 25 °C /22 °C , respectively, with a relative humidity of 40%). The roots, stems,
131 leaves, flowers and seeds at different developing stages were collected (Sd1-Sd3 represent prophase,
132 mid-term, later period of ovary bulge, Sd4-Sd6 represent prophase, mid-term, later period of grout,
133 and Sd7-Sd9 represent prophase, mid-term, later period of mature); these samples were immediately
134 frozen in liquid nitrogen, and stored at -80 °C for further use. Sterile seeds of *F. tataricum* were
135 grown on Murashige and Skoog medium (MS) after soaking in warm water (37 °C) for 20 min. The
136 substrates tested in the present study were purchased from Xili Limited Co. (Shanghai, China) and
137 Indofine (Hillsborough, NJ, USA). UDP-glucose and UDP-glucuronic acid were purchased from
138 Sigma-Aldrich (Oakville, CA, USA). UDP-rhamnose was enzymatic synthesized using methods
139 mentioned in Rautengarten et al. (2014). Chemicals used in this study were all of analytical or
140 HPLC grade.

141

142 **2.2 RNA extraction, sequencing and reads filtering**

143

144 In order to examine the expression patterns of FtUGT genes associated with rutin and emodin
145 glycosides biosynthetic pathway, RNAs from leaves, roots, stems, flowers and seeds of different
146 developing stages were sequenced by Illumina HiSeq2000 platform. High-quality RNA was
147 separately extracted from the fresh samples of *F. tataricum* using TaKaRa MiniBEST Plant RNA
148 Extraction Kit. Libraries were constructed following the manufacturer's instructions, and sequence
149 was carried out by using the Illumina HiSeq2000 platform. The raw reads were filtered following
150 the same parameters, which used the Custom Perl script to generate contigs' database (Ravi &
151 Mukash, 2012), and finally resulted in a total of ~37.4 Gb clean data. RNA-Seq reads from each
152 tissue were individually mapped to the annotated genes from published genome of *F. tataricum*

153 (Trapnell *et al.* 2017) with default parameters. The expression level of each gene was evaluated by
154 Fragments Per Kilobase per Million mapped fragments (FPKM) and calculated using Tophat and
155 Cufflinks (version 2.1.1) with default parameters (Trapnell *et al.* 2017).

156

157 **2.3 Isolation and sequence analysis of FtUGTs**

158

159 Primers for the 14 FtUGT genes were designed according to the published genome of *F. tartaricum*.
160 All the forward and reverse primers (see Supplementary Data S3) for gene cloning contained
161 corresponding restriction sites. Mixed cDNAs from root, stem, leaves and seeds of *F. tartaricum*
162 were used for gene amplification. The PCR products were purified and digested using the
163 corresponding restriction enzymes, and then ligated to the pMAL-c2x vector (New England
164 BioLabs, Ipswich, MA, USA) digested with the same restriction enzymes for expression of
165 recombinant protein in *Escherichia coli*.

166

167 Multiple sequence alignment of the deduced amino acid sequences was carried out by using
168 DNASTAR. Predicted amino acid sequences of UGTs were aligned using Clustal X2 and further
169 used for phylogenetic analysis. The neighbor-joining phylogenetic tree was constructed with 1000
170 boot-strap replicates using MEGA4.0 software (Tamura, Dudley, Nei, & Kumar, 2007).

171

172 **2.4 Enzyme assay and product identification**

173

174 Gaining recombinant UGT proteins in *E. coli* was followed as previously described (Yin *et al.*,
175 2017); the crude proteins were used to enzymatic activity test. Optimal temperature for
176 FtUGT73BE5 was measured in 50 mM Tris-HCl (pH 7.0) with 2.5 μ g purified protein, 2 mM
177 UDP-glucose, 10 mM DTT and 100 μ M quercetin or emodin, under temperature from 25 to 50°C.

178 To assess the optimal pH, the recombinant protein was put in the 50 mM Tris-HCl (pH 6, pH 7 or
179 pH 8) on 37 °C . The substrate specificity of FtUGT73BE5 was analyzed with 100 μ M candidate
180 flavonoids and emodin for 30 minutes on 37 °C . For kinetic analysis of the recombinant
181 FtUGT73BE5 protein, purified enzymes (10 μ g) were incubated in reaction mixtures comprising 10
182 mM DTT, 50 mM Tris-HCl (pH 7.0), and 2 mM UDP-glucose or UDP-glucuronic acid or
183 UDP-rhamnose crude (20 μ l enzymatic solution with UDP-rhamnose), in a final volume of 100 μ l.
184 The concentration of the tested acceptor substrates ranged from 0 to 400 μ M. Reactions were
185 stopped by addition of methanol after 30 min incubation at 37 °C . Samples were centrifuged at 14,
186 000 rpm for 10 min at 4 °C , and further analyzed by HPLC or UPLC. The kinetic parameters K_m
187 and K_{cat} were calculated by using the Hyper 32 program (<http://hyper32.software.informer.com/>).
188
189 Enzymatic reaction solution was filtered through 0.22 μ m membranes, 20 μ L aliquot was used to
190 analyse the new products by HPLC (Yin *et al.*, 2017), then a 1 μ L aliquot was injected into
191 UPLC-MS/MS for identifying the products. A 1290 series UPLC was coupled with a 6470 triple
192 quadrupole mass spectrometer via an AJS-ESI interface (Agilent Technologies, Waldbronn,
193 Germany). Samples were eluted on an Agilent Eclipse Plus C18 column (RRHD 1.8 μ m, 2.1 \times 50
194 mm). Acetonitrile was used as mobile phase A, water solution containing 0.1% formic acid and 0.1%
195 ammonium formate was used as mobile phase B. The analytes were eluted using a linear gradient
196 program: 0~12 min, 95% \rightarrow 5% B and washed for 1 min. The flow rate was 0.20 ml min⁻¹ and
197 column temperature was 45 °C . Mass spectrometer was operated in negative ion mode, with sheath
198 gas temperature at 300 °C , gas flow at 5.0 L min⁻¹, and nebulizer gas at 45 psi. Capillary voltage was
199 set at 3500 V, nozzle voltage 500 V, and delta EMV 200 V. Product Ion mode was used, and two
200 precursor-product ions were selected for the qualification of glycosylated products, as shown in

201 Supplementary Table S3. Quantity data for all flavonol and emodin metabolites was analyzed by
202 MassHunter (version B.07.00).

203

204 **2.5 Homology modeling and docking statistic**

205

206 Homology models of the FtUGT73BE5 were built, using the 3D structure of UGT84A1 (The
207 UniProt Knowledgebase: Q5XF20) as a template, with the SWISS-MODEL server at
208 <http://swissmodel.expasy.org> (Biasini *et al.*, 2014). The amino acid sequence identity between
209 FtUGT73BE5 protein and UGT84A1 was 40%. UDP-Glucose and quercetin 3-*O*-glucoside were
210 respectively docking with the model structure of FtUGT73BE5 using the Igemdock 2.1 program.
211 The docking result with UDP-Glucose and quercetin 3-*O*-glucoside was visualized with the Pymol
212 molecular graphics system at <http://www.pymol.org>.

213

214 **2.6 Expression analysis by quantitative real-time PCR**

215

216 Total RNA was isolated from roots, stems, leaves, flowers, and developing seeds of *F. tataricum* by
217 using an RNAprep Pure Plant Kit (Tiangen Biotech Co., Beijing, China). The *histone H3 (His3*
218 *gene)* was used as a housekeeping gene in qRT-PCRs (Zhou *et al.*, 2016).

219

220 Total RNA from UGT-overexpression or -knockdown hairy roots were extracted. PCR system was
221 the same as previously described (Yin *et al.*, 2017). Primer sequences used for qRT-PCR were listed
222 in Supplementary Data S2.

223

224 **2.7 Treatment of *F. tataricum* s with hormones**

225

226 The cotyledons from one week seedlings of *F. tataricum* were collected, and then soaked in water
227 with DMSO (100 μ M), Me-jasmonic acid (MeJA; 100 μ M) and abscisic acid (ABA; 100 μ M) for 4,
228 14, and 24 h in dark, respectively. The samples were harvested and immediately frozen in liquid
229 nitrogen, and stored at -80°C until use.

230

231 **2.8 Overexpression and knockdown *FtUGT73BE5* in *F. tataricum* hairy root**

232

233 To investigate whether *FtUGT73BE5* has the same catalytic activity toward quercetin and emodin
234 *in vivo* as observed *in vitro*, the plasmids for overexpression and RNA interference (RNAi) of
235 *FtUGT73BE5* were constructed by Gateway system (Invitrogen Corporation). Briefly speaking, the
236 ORF region of the *FtUGT73BE5* driven by 35S CaMV promoter was subcloned to the binary vector
237 pK7WG2D for gene overexpressing in plant, while the specific fragment about 300bp length of the
238 *FtUGT73BE5* was cloned to the binary vector pK7GWIWG2II2D for RNAi. The resulting
239 overexpression (pK7WG2D-*FtUGT73BE5*) and RNAi (pK7GWIWG2II2D-*FtUGT73BE5*)
240 constructs were transformed into *Agrobacterium ATCC 10060* to generate transgenic hairy roots of
241 *F. tataricum*.

242

243 The generation of tartary buckwheat hairy root was operated as before (Zhang *et al.*, 2019). After
244 selecting for one week, GFP signal was detected under a fluorescent display instrument. The
245 transgenic hairy roots were further cultured in B5 liquid medium with the same antibiotics for
246 another three weeks in flask before harvest. Finally, the hairy root samples were used for qRT-PCR,
247 flavonol and emodin metabolites analysis. In order to investigate whether *FtUGT73BE5* has the
248 same catalytic activity toward emodin *in vivo*, emodin (final concentration was 100 μ M) was added
249 to the B5 liquid medium, co-cultured with transgenic hairy roots for 24 h as similar to before due to
250 the reason of emodin can hardly be detected in hairy roots of *F. tataricum* (Karimi *et al.*, 2002).

251
252 **2.9 Analysis of flavonol and emodin metabolites by UPLC/MS/MS**

253
254 The *FtUGT73BE5* overexpression and knockdown hairy root lines were selected and extracted for
255 flavonol and emodin analysis by UPLC/MS/MS. 10 mg dry weight sample was extracted with 1 ml
256 methanol in an ultrasonic bath at 25 °C for 30 min. Then the supernatant was filtered through a
257 membrane (pore diameter is 0.22 μm) after centrifuging 10 min (12, 000 rpm) under 4 °C. Finally, a
258 1 μl aliquot was injected into UPLC/MS/MS for subsequently analysis. The UPLC/MS/MS method
259 was the same as mentioned above in 2.6: metabolites were detected in multiple reaction monitoring
260 (MRM) mode, the MRM transitions of two precursor-product ion were selected as references for
261 each compound, as shown in Table S3. Data was analyzed by MassHunter (version B.07.00).

262
263 **2.10 Statistical analysis**

264
265 Statistical analyses were performed using Excel (Microsoft Office, Microsoft). P-values were
266 calculated using an unpaired, two-legged Student's *t* test (** $p < 0.01$; * $p < 0.05$; ns, not significant).
267 Data represent means \pm standard deviation ($n \geq 3$).

268
269 **3 Results and discussions**

270
271 **3.1 Characteristics of FtUGT genes in *F. tataricum* genome**

272
273 With the help of the UGT nomenclature committee, the submitted 106 UGT genes were named;
274 proteins encoded by these genes are comprise of 300 to 600 amino acids, and have significant PSPG
275 motifs near their C-terminals (Data S1). Our analysis revealed that 38 of the 106 FtUGT genes

276 contained no introns, while 48 FtUGTs contained only a single intron (Fig.S2). The number of
277 FtUGTs without intron (38 out of 106) is apparent small than that of other plants, such as peach (72
278 out of 168) (Wu *et al.*, 2017). Their physical locations mapped on 8 chromosomes with a relatively
279 high density on the chromosome 1 (14 FtUGTs), 6 (16 FtUGTs), 7 (18 FtUGTs) and 8 (15 FtUGTs)
280 (Fig.S3).

281

282 We constructed a phylogenetic tree with these 106 FtUGTs and 119 AtUGTs (Fig. 1). According to
283 the phylogenetic tree, FtUGTs clustered into 23 families, 14 evolutionary groups (A-H, J-N, and P)
284 and an uncharacterized group. Even though the number of groups become less, a new and an
285 unclassified one (UGT93 family and UGT95 family) were emerged comparing to AtUGTs. Seven
286 groups cover 77% members of FtUGTs: E (15), B (14), G (13), H (12), D (11), L (9) and A (8) (Fig.
287 1). Several UGTs in other plant, belonged to A, B, D, E, F, G and L evolutionary groups, had been
288 reported to involve in flavonoid or emodin glycosylation. LjUGT72AD1 and LjUGT72Z2 from
289 group E were identified to glycosylate flavonol in *L. japonicas* hairy root (Yin *et al.*, 2017).
290 GmUGT79A6 (*G. max*) and FeUGT79A8 belonged to group A were reported to involve in rutin
291 biosynthesis (Rodas *et al.*, 2014; Koja *et al.*, 2018). Therefore, in this study, FtUGTs sorted to
292 group A, B, D, E, F, G and L were preferentially chosen to be further investigated.

293

294 **3.2 Expression profiles of UGT genes in *F. tataricum***

295

296 We retrieved the expression profiles of 106 full-length UGT genes from transcriptome of *F.*
297 *tataricum* (Fig. 2 and Data S2). Hierarchical clustering analysis of the transcript data indicated that
298 57 UGT genes expressed in developing seeds. Among them, 20 UGT genes possessed high
299 expression levels in late development stage of seeds, other 31 UGT genes were highly expressed at
300 the stage of ovary bulge, while six UGT genes were highly expressed at the stage of ovary bulge

301 and seed maturation. Furthermore, in total of 11, 23 and 11 UGT genes were highly expressed in
302 roots, stems, and leaves, respectively.

303

304 Due to the expression profiles, the evolutionary analysis and UGT family identification related to
305 flavonoid or emodin in other species, total 19 FtUGTs were selected for their high expression in
306 seed and close relationship with flavonoids and emodin glycosylations. These candidates include
307 family UGT79s in group A, UGT89s in group B, UGT73s in group D, UGT71s, UGT72s and
308 UGT88s in group E, UGT714s in group F, UGT85s in group G and UGT75s and UGT84s in group
309 L (Table S1) (Dhaubhadel, Farhangkhoe, & Chapman, 2008, Xie *et al.*, 2014, Funaki *et al.*, 2015,
310 Yin *et al.*, 2017). Two FtUGTs from unclassified group were also screened for their expression
311 pattern; FtUGT93R1 was highly expressed in roots and seeds, while FtUGT95D1 was top one in
312 expression level among all UGTs in roots, leaves and seeds. Finally, 21 FtUGTs were selected as
313 candidates according to phylogenetic tree and transcriptomics analysis.

314

315 **3.3 Sequence analyses and enzymatic activity of FtUGTs**

316

317 Comparing to the sequences of reported functional UGTs toward flavonoids and emodin, 21
318 candidate FtUGTs were distributed into five clusters in an unrooted phylogenetic tree, that is in
319 3GT (1 FtUGT), 5GT (8), 7GT (4), CGT (6) and Branch forming clusters (2); while FtUGT95D1
320 located in an independent cluster (Fig. S4A). Fourteen FtUGTs out of 21 candidates were cloned
321 and expressed in *E. coli* to produce recombinant proteins to investigate their enzymatic activities
322 eventually. These 14 putative FtUGTs shared a relatively high identity within the PSPG box with
323 'W-2x-Q-3x-L-8x-H-x-G-2x-S-2x-E-17x-Q' motif near their C-terminal ends; FtUGT714C1
324 composed of 45 amino acids in its PSPG box, differed from other FtUGTs, which possessed 44
325 amino acids in PSPG box (Fig. S4B & S4C). Their open reading frames ranged from 1257 bp to

326 1548 bp in length encoding proteins from 419 to 515 amino acids. The last amino acids in their
327 PSPG box were all glutamine (Q), suggesting that they may use UDP-glucose as sugar donor like
328 previously reported UGT proteins (Kubo, Arai, Nagashima, & Yoshikawa, 2004).

329

330 Enzymatic tests were carried out by using 11 flavonoids like aglycones and emodin as sugar
331 acceptors, and using UDP-glucose, UDP-glucuronic acid and UDP-rhamnose as sugar donors (Fig.
332 S4C). Our results revealed that recombinant UGT73BE5 (rUGT73BE5), rUGT75R2, rUGT75R3,
333 rUGT85AD3, and rUGT89G2 could use quercetin as substrate, while rUGT73BE5, rUGT75R2 and
334 rUGT75R3 could use emodin as substrate; these five UGTs could use UDP-glucose but not
335 UDP-glucuronic acid or UDP-rhamnose as sugar donor (Fig. 3A; Table S2). Among them,
336 rUGT73BE5 and rUGT75R2 also showed glucosylate activity toward quercetin 3-*O*-glucoside.
337 Further test of rUGT73BE5 and rUGT75R2 to seven other substrates showed that rUGT73BE5
338 possessed more complex substrate diversity than rUGT75R2 (Table S2).

339

340 Our data revealed that all of these enzymatic products were characterized as addition of one or two
341 glucoses (molecular weight increased 162 or 324) to yield their corresponding aglycones (Fig.3B).
342 The enzymatic products of rFtUGT73BE5 with quercetin substrate included quercetin
343 3-*O*-glucoside and quercetin di-glucoside comparing with authentic standards (Fig. 3B).
344 Furthermore, when quercetin 3-*O*-glucoside was used as substrate, the enzymatic products were
345 identified as two new quercetin di-glucosides by MS (Fig.3A and 3C). Similarly, FtUGT73BE5
346 could catalyze luteolin and kaempferol to form their di-glucoside (Fig. S5). Enzymatic products of
347 FtUGT73BE5 with other tested substrates were all mono-glycoside confirmed by MS (Fig. S5).
348 FtUGT75R2 could also catalyze quercetin to produce quercetin monoglucoside and di-glucoside,
349 while merely catalyze other substrates to produce mono-glucoside (Fig. S6). Since we mainly
350 focused on the procedure from quercetin to quercetin 3-*O*-glucoside, the glycosylated position of
351 these di-glucosides was not identified further.

352

353 The enzymatic products of rUGT73BE5, rUGT75R2 and rUGT75R3 with emodin substrate were
354 predicted as emodin 6-*O*-glucoside, as compared with authentic standards of emodin 1-*O*-glucoside
355 and emodin 8-*O*-glucoside (Fig. 3D & 3E, Fig. S7). A previous work reported that some kind of *E.*
356 *coli* could produce emodin glycoside mixtures including emodin 6-*O*-glucoside and emodin
357 8-*O*-glucoside, but which protein contributed to these procedures was not stated (Zhang, Ye, Zhan,
358 Chen, & Guo, 2004). The majority enzymatic product of FtUGT73BE5 was emodin 6-*O*-glucoside,
359 with extremely minor emodin 8-*O*-glucoside detected by UPLC-QQQ, which differing from
360 CtUGT73AE1 mainly catalyzing emodin to form 8-*O*-glucoside (Xie *et al.*, 2014). Moreover,
361 CtUGT73AE1 was observed to catalyze the reversible glycosyltransferase reactions, which could be
362 employed for deglycosylation to form UDP-glucose in certain cases. Since FtUGT73BE5 shares 43%
363 amino acids identity with CtUGT73AE1, whether it has similar reversing glycosylation ability
364 might to be investigated in the future.

365

366 We further studied the characteristics of rFtUGT73BE5, including optimum pH value, optimum
367 enzymatic temperature, substrate specificity and enzymatic kinetic properties (Fig S8 and Fig. 4A &
368 4B). Among 6.0 to 8.0, the optimum pH value for producing quercetin and emodin were both 7.0.
369 The enzymatic ability were enhanced with the increasing of temperature from 25 °C to 50 °C. The
370 optimum enzymatic ability for quercetin was 190.5 *pkat*/mg protein at 50 °C, while that was 170
371 *pkat*/mg protein for emodin (Fig S8 A&B). The reaction rate for quercetin was 99.8 *pkat*/mg protein
372 and for emodin was 88.8 *pkat*/mg protein, which both were the highest in the 10 tested substrates
373 except for naringenin (127.6 *pkat*/mg protein) and luteolin (268.8 *pkat*/mg protein) (Fig S8 C).

374

375 Enzymatic kinetic test showed that the affinity of rUGT73BE5 for kaempferol (40.26 μ M) and
376 quercetin 3-*O*-glucoside (22.42 μ M) was stronger than that for quercetin and emodin. The high

377 K_{cat}/K_m values for kaempferol and quercetin 3-*O*-glucoside were $0.53 \times 10^{-3} \text{ s}^{-1} \mu\text{M}^{-1}$ and 0.47×10^{-3}
378 $\text{s}^{-1} \mu\text{M}^{-1}$, respectively. These results indicated that rFtUGT73BE5 was more efficient toward
379 quercetin 3-*O*-glucoside than other substrates. Phylogenetic analysis demonstrated that
380 FtUGT73BE5 was clustered into 7-*O*-group; however our enzymatic study showed that it possessed
381 multiple functions toward different substrates with different positions. These results suggested that
382 the correlation between amino acid similarity of glycosyltransferases and their functions was not
383 strong (Chang, Singh, Phillips, & Thorson, 2011). Therefore, predicting function by protein
384 structure would be more practical than amino acids sequence alignment (Sharma, Panigrahi, &
385 Suresh, 2014). To explore the potential molecular basis for the highly enzymatic activity of
386 FtUGT73BE5 towards quercetin 3-*O*-glucoside, we analyzed the interactions between amino acid
387 residues and the substrates, including quercetin 3-*O*-glucoside and UDP-glucose. This analysis
388 predicted the interaction between ten amino acids (His17, Gly18, Cys287, Gln355, His370, Trp373,
389 Asn374, Ser375, Glu394 and Gln395) and the sugar donor UDP-glucose in FtUGT73BE5 by
390 H-bond. Moreover, other ten amino acids (Gly18, His19, Gly140, Ser141, Cys287, Ser290, Gln355,
391 Asn374, Ser375 and Glu394) could potentially form H-bond with quercetin 3-*O*-glucoside (Fig. 4C).
392 The docking results suggested that the ligand-bindings on FtUGT73BE5 in a central cleft were
393 formed by the N- and C-terminal domains (Fig. 4C); it was big enough to hold both quercetin
394 3-*O*-glucoside and UDP-glucose, which could explain why rFtUGT73BE5 possesses high catalyzed
395 activity for quercetin 3-*O*-glucoside.

396

397 **3.4 *In vivo* function of FtUGT in *F. tataricum* hairy roots**

398

399 In order to evaluate the *in vivo* functions of FtUGT73BE5, we carried out overexpression driven by
400 35S promoter and knockdown through RNA interference (RNAi) in *F. tataricum* hairy root via
401 *Agrobacterium rhizogenes*-mediated transformation. At least 10 transgenic hairy root lines were

402 obtained; qRT-PCR was used to quantify expression levels in over-expression and RNAi lines (Fig.
403 5A & 5B and Fig. S9A).

404

405 Compared to control, rutin content increased from 0.77 to 1.29-fold in three *FtUGT73BE5*
406 over-expression transgenic lines (Fig. 5C). The intermediate quercetin 3-*O*-glucoside increased
407 from 0.32- to 1.15-fold compare to control (Fig. 5C). The results appeared in *FtUGT73BE5*
408 knockdown lines were coincided. Compared to control, quercetin 3-*O*-glucoside decreased from
409 0.6- to 0.65-fold while rutin content similarly decreased from 0.54- to 0.64-fold in three
410 *FtUGT73BE5* RNA interference lines (Fig. S9B & C). These results demonstrated that
411 *FtUGT73BE5* could catalyze the formation of rutin and quercetin 3-*O*-glucoside *in vivo*.

412

413 Since emodin and emodin glucosides were hardly detected in *F. tataricum* hairy root, the function
414 of *FtUGT73BE5* was verified by feeding emodin substrate to transgenic hairy roots (Fig. 5D & 5E).
415 The result indicated that emodin 6-*O*-glucoside was mainly detected in *FtUGT73BE5*
416 over-expressing hairy roots; the content of emodin 6-*O*-glucoside in these overexpression lines was
417 significantly higher than that in the control line, ranging from 17.36- to 22.73-fold. These results
418 suggested that *FtUGT73BE5* could glucosylate emodin to produce emodin 6-*O*-glucoside in *F.*
419 *tataricum* hairy root .

420

421 As a superfamily, the UGT functions possess quite diversity and redundancy, which makes them
422 difficult to identify in native species. In model plants, such as citrus, strawberry, Medicago, soybean
423 and *L. japonicus*, their UGT functions were commonly found verifying in native plants (Frydman et
424 al. 2004; Griesser et al. 2008; Pang, Peel, Sharma, Tang, & Dixon, 2008; Kojas et al. 2014; Yin et
425 al. 2017). A few researches had focus on buckwheat UGTs: FeCGTa and FeCGTb were confirmed
426 to have C-glucosylation activity toward flavonoids *in vitro* (Nagatomo *et al.* 2014); FeUGT79A8
427 was identified to rhamnosylate quercetin 3-*O*-glucoside in tobacco(Kojas et al. 2018); three *FtUGTs*

428 were identified to involve in anthocyanidin glucosylation *in vitro* (Zhou et al. 2016). Differently, in
429 our study FtUGT73BE5 was illustrated could glucosylate quercetin and emodin not only *in vitro*
430 through enzymatic tests, but also in native plants.

431

432

433 **3.5 The expression pattern of *FtUGT73BE5* and its relationship with hormone**

434

435 In order to characterize the function of *FtUGT73BE5* in plant, we further analyzed their expression
436 levels in various tissues and different developing stages of seeds using qRT-PCR, *FtUGT75R2* was
437 selected as control (Fig. 6A). The expression patterns of the two FtUGTs were similar with the data
438 from transcriptome; *FtUGT73BE5* was highly expressed in leaves and seeds of *F. tataricum*, which
439 consisted with the accumulation trends of rutin in these tissues. This result further confirmed that
440 FtUGT73BE5 was truly responsible for the biosynthesis of rutin in leaves and seeds of *F. tataricum*
441 (Fig. 6A). The transcript level of FtUGT73BE5 was down-regulated in the procedure of seed
442 maturation; these may be caused by the accumulation of ABA at the mature stage of seeds.

443

444 Rutin was produced when plants suffer from adversity (Zhou et al., 2016). In our study, the rutin
445 content increased about 5% after treated with ABA or MeJA, despite it reached as high as 34.9
446 mg/g dry weight in the cotyledon (Fig. 6B & C).

447

448 A previous study indicated that ABA and MeJA induced the expression of *LjUGT72AD2* and
449 *LjUGT72Z1* from *L. japonicas*, which encoding two flavonol *O*-glucosyltransferases (Yin *et al.*,
450 2017). Similarly, the transcription of *FtUGT73BE5* was induced by MeJA for more than 4.26-fold
451 after 14 h comparing to control (Fig. 6B). Conversely, after treated with ABA, the transcription of
452 *FtUGT73BE5* was depressed by 0.17-fold after 5 h compared with untreated controls (Fig. 6B).

453 These experimental results demonstrated that ABA could inhibit the expression of FtUGT73BE5,
454 which was coincided with the expression trend of FtUGT73BE5 in mature seeds.

455

456 4 Conclusion

457

458 In this study, 106 FtUGTs were systematically and comprehensively analyzed in genome level,
459 from gene structure, chromosome location to phylogenetic category of encoding proteins. Even
460 though less total number, FtUGTs formed a new evolutionary group and an unclassified group
461 (UGT93 family and UGT95 family) comparing with AtUGTs. The transcript profiles of FtUGTs in
462 different temporal and spatial stages were analyzed. Almost half of total FtUGT genes (57 UGTs)
463 were highly expressed in developing seeds.

464

465 A glucosyltransferase FtUGT73BE5 was identified involving to glucosylate rutin and emodin *in*
466 *vitro* and *in vivo*. Among 21 candidate FtUGTs, screened based on published tartary buckwheat
467 genome and their spatial and temporal transcripts, FtUGT73BE5 and others 4 FtUGTs were
468 identified to glucosylate flavonol or emodin *in vitro*. rFtUGT73BE5 especially possessing substrate
469 diversity could catalyze glucosylation of all tested flavonoids and emodin. Furthermore, the
470 functions of FtUGT73BE5 *in vivo* were demonstrated in hairy roots of tartary buckwheat. Rutin
471 content was increased at most by 1.29-fold in *FtUGT73BE5* over-expressing lines, while the
472 emodin 6-*O*-glucoside content was increased at most by 22.73-fold in transgenic lines when
473 supplying emodin substrate.

474

475 The transcript profile of *FtUGT73BE5* was consistent with the accumulation trend of rutin in plant.
476 It may relate to anti-adversity for its transcript level was up-regulated by MeJA, but repressed by
477 ABA. Our work about glycosylation for rutin and emodin glucosides in tartary buckwheat not only

478 illuminates their biosynthetic pathway and biological interests, but also provides a theory basis for
479 developing healthy food products with tartary buckwheat.

480

481 **Acknowledgements**

482

483 Illumina sequencing was done at Novogene co. ltd. This research was supported by Beijing Natural
484 Science Foundation (7192138), the National Natural Science Foundation of China (81703647,
485 31471562), the Fundamental Research Funds for the Central public welfare research institutes
486 (ZZ13-YQ-097), National Key R&D Program of China (2019YFC1711100), and National Science
487 and Technology Major Project "Creation of Major New Drugs" (2019ZX09201005-006-004, No.
488 2019ZX09731-002).

489

490 **Accession numbers**

491

492 The GenBank accession numbers of sequences for this research as follow, FtUGT714C1,
493 MH197430; FtUGT85A68, MH197422, FtUGT85A66, MH197421; FtUGT75R3, MH197425;
494 FtUGT75R2, MH197426; FtUGT89G2, MH197419; FtUGT95D1, MH197417; FtUGT73E11,
495 MH197413; FtUGT85AC1, MH197420; FtUGT79J1, MH197416; FtUGT73BE5, MH197414;
496 FtUGT85AD3, MH197423; FtUGT85AD1, MH197424; FtUGT93R1, MH197429. SRA accession
497 of transcripts data from different tissues of *F. tataricum*: SRP141278.

498

499 **References**

500 AL-Snafi, A.E. (2017). Therapeutic importance of *Ephedra alata* and *Ephedra foliate*. *Indo*
501 *American Journal of Pharmaceutical Sciences*, 4, 399-406.

- 502 An, D.G., Yang, S.M., Kim, B.G., & Ahn, J.H. (2016). Biosynthesis of two quercetin
503 *O*-diglycosides in *Escherichia coli*. *Journal of Industrial Microbiology & Biotechnology*, 43,
504 841-849.
- 505 Bringmann, G., & Irmer, A. (2008). Acetogenic anthraquinones: biosynthetic convergence and
506 chemical evidence of enzymatic cooperation in nature. *Phytochemistry Reviews*, 7, 499-511.
- 507 Biasini, M., Bienert, S., Waterhouse, A., Arnold, K., Studer, G., Schmidt, T., Kiefer, F., Cassarino,
508 T.G., Bertoni, M., Bordoli, L., & Schwede, T. (2014). SWISS-MODEL: modelling protein
509 tertiary and quaternary structure using evolutionary information. *Nucleic Acids Research*, 42,
510 W252-W258.
- 511 Caputi, L., Malnoy, M., Goremykin, V., Nikiforova, S., & Martens, S. (2012). A genome-wide
512 phylogenetic reconstruction of family 1 UDP-glycosyltransferases revealed the expansion of
513 the family during the adaptation of plants to life on land. *The Plant Journal*, 69, 1030-1042.
- 514 Chang, A., Singh, S., Phillips, G.N., Jr., & Thorson, J.S. (2011). Glycosyltransferase structural
515 biology and its role in the design of catalysts for glycosylation. *Current Opinion in*
516 *Biotechnology*, 22, 800-808.
- 517 Chen, Q.F. (2018). The status of buckwheat production and recent progresses of breeding on new
518 type of cultivated buckwheat. *Journal of Guizhou Normal University Natural Sciences*, 362,
519 1-7.
- 520 Dhaubhadel, S., Farhangkhome, M., & Chapman, R. (2008). Identification and characterization of
521 isoflavonoid specific glycosyltransferase and malonyltransferase from soybean seeds. *Journal*
522 *of Experimental Botany*, 59, 981-994.
- 523 Fabjan, N., Rode, J., Kosir, I.J., Wang, Z., Zhang, Z., & Kreft, I. (2003). Tartary buckwheat
524 *Fagopyrum tataricum* Gaertn. as a source of dietary rutin and quercitrin. *Journal of*
525 *Agricultural and Food Chemistry*, 51, 6452-6455.
- 526 Frydman, A., Weisshaus, O., Bar-Peled, M., Huhman, D.V., Sumner, L.W., Marin, F.R., Lewinsohn,
527 E., Fluhr, R., Gressel, J., & Eyal, Y. (2004). Citrus fruit bitter flavors: isolation and functional

- 528 characterization of the gene Cml_{1,2}RhaI encoding a 1,2 rhamnosyltransferase, a key enzyme
529 in the biosynthesis of the bitter flavonoids of citrus. *The Plant Journal*, 40, 88-100.
- 530 Funaki, A., Waki, T., Noguchi, A., Kawai, Y., Yamashita, S., Takahashi, S., & Nakayama, T.
531 (2015). Identification of a highly specific isoflavone 7-*O*-glucosyltransferase in the soybean
532 *Glycine max* (L.) Merr. *Plant and Cell Physiology*, 56, 1512-1520.
- 533 Ghimire, G.P., Koirala, N., Pandey, R.P., Jung, H.J., & Sohng, J.K. (2015). Modification of emodin
534 and aloe-emodin by glycosylation in engineered *Escherihia coli*. *World Journal of*
535 *Microbiology and Biotechnology*, 31, 611-619.
- 536 Griesser, M., Vitzthum, F., Fink, B., Bellido, M.L., Raasch, C., Munoz-Blanco, J., & Schwab, W.
537 (2008). Multi-substrate flavonol *O*-glucosyltransferases from strawberry *Fragaria x ananassa*.
538 achene and receptacle. *Journal of Experimental Botany*, 59, 2611-2625.
- 539 Jing, R., Li, H.Q., Hu, C.L., Jiang, Y.P., Qin, L.P., & Zheng, C.J. (2016). Phytochemical and
540 pharmacological profiles of three Fagopyrum Buckwheats. *International Journal of Molecular*
541 *Sciences*, 17, E589.
- 542 Koja, E., Ohata, S., Maruyama, Y., Suzuki, H., Shimosaka, M., & Taguchi, G. (2018).
543 Identification and characterization of a rhamnosyltransferase involved in rutin biosynthesis in
544 *Fagopyrum esculentum* (common buckwheat). *Bioscience Biotechnology and Biochemistry*, 4,
545 1-13.
- 546 Kovinich, N., Saleem, A., Arnason, J.T., & Miki, B. (2010). Functional characterization of a
547 UDP-glucose:flavonoid 3-*O*-glucosyltransferase from the seed coat of black soybean *Glycine*
548 *max* L. Merr. *Phytochemistry*, 71, 1253-1263.
- 549 Kubo, A., Arai, Y., Nagashima, S., & Yoshikawa, T. (2004). Alteration of sugar donor specificities
550 of plant glycosyltransferases by a single point mutation. *Archives of Biochemistry and*
551 *Biophysics*, 429, 198-203.
- 552 Lee, W., Ku, S.K. & Bae, J.S. (2013). Emodin-6-*O*- β -D-glucoside down-regulates endothelial
553 protein C receptor shedding. *Archives of Pharmacal Research*, 36, 1160-1165.

- 554 Liu, C.L., Chen, Y.S., Yang, J.H., & Chiang, B.H. (2008). Antioxidant activity of Tartary
555 *Fagopyrum tataricum* (L.) Gaertn. and common *Fagopyrum esculentum* Moench. buckwheat
556 sprouts. *Journal of Agricultural and Food Chemistry*, *56*, 173-178.
- 557 Mizohata, E., Okuda, T., Hatanaka, S., Nakayama, T., Horikawa, M., Nakayama, T., Ono, E., &
558 Inoue, T. (2013). Crystallization and preliminary X-ray crystallographic analysis of
559 UDP-glucuronic acid:flavonol-3-*O*-glucuronosyltransferase VvGT5 from the grapevine *Vitis*
560 *vinifera*. *Acta Crystallographica Section F Structural Biology Communications*, *69*, 65-68.
- 561 Nagatomo, Y., Usui, S., Ito, T., Kato, A., Shimosaka, M., & Taguchi, G. (2014). Purification,
562 molecular cloning and functional characterization of flavonoid C-glucosyltransferases from
563 *Fagopyrum esculentum* M. buckwheat. cotyledon. *The Plant Journal*, *80*, 437-448.
- 564 Owens, D.K., & McIntosh, C.A. (2009). Identification, recombinant expression, and biochemical
565 characterization of a flavonol 3-*O*-glucosyltransferase clone from *Citrus paradisi*.
566 *Phytochemistry*, *70*, 1382-1391.
- 567 Pang, Y.Z., Peel, G.J., Sharma, S.B., Tang, Y.H., & Dixon, R.A. (2008). A transcript profiling
568 approach reveals an epicatechin-specific glucosyltransferase expressed in the seed coat of
569 *Medicago truncatula*. *Proceedings of the National Academy of Sciences of the United States of*
570 *America*, *105*, 14210-14215.
- 571 Peng, L.X., Wang, J.B., Hu, L.X., Zhao, J.L., Xiang, D.B., Zou, L., & Zhao, G. (2013). Rapid and
572 simple method for the determination of emodin in Tartary buckwheat *Fagopyrum tataricum*.
573 by high-Performance liquid chromatography coupled to a diode array detector. *Journal of*
574 *Agricultural and Food Chemistry*, *61*, 854-857.
- 575 Ravi, K.P., & Mukash, G. (2012). NGS QC Toolkit: a toolkit for quality control of next generation
576 sequencing data. *PLoS One*, *7*, e30619.
- 577 Rautengarten, C., Ebert, B., Moreno, I., Temple, H., Herter, T., Link, B., Doñas-Cofré, D., Moreno,
578 A., Saéz-Aguayo, S., Blanco, F., Mortimer, J.C., Schultink, A., Reiter, W. D., Dupree, P.,
579 Pauly, M., Heazlewood, J.L., Scheller, H.V., & Orellana, A. (2014) The Golgi localized

- 580 bifunctional UDP-rhamnose/UDP-galactose transporter family of Arabidopsis. *Proceedings of*
581 *the National Academy of Sciences of the United States of America*, *111*, 11563-11568.
- 582 Rodas, F.R., Rodriguez, T.O., Murai, Y., Iwashina, T., Sugawara, S., Suzuki, M., Nakabayashi, R.,
583 Yonekura-Sakakibara, K., Saito, K., Kitajima, J., Toda, K., & Takahashi, R. (2014). Linkage
584 mapping, molecular cloning and functional analysis of soybean gene *Fg2* encoding flavonol
585 3-*O*-glucoside 1 \rightarrow 6. rhamnosyltransferase. *Plant Molecular Biology*, *84*, 287-300.
- 586 Sharma, R., Panigrahi, P., & Suresh, C.G. (2014). In-silico analysis of binding site features and
587 substrate selectivity in plant flavonoid-3-*O* glycosyltransferases F3GT through molecular
588 modeling, docking and dynamics simulation studies. *Plos One*, *9*, e92636.
- 589 Sun, W., Leng, L., Yin, Q., Xu, M., Huang, M., Xu, Z., Zhang, Y., Yao, H., Wang, C., Xiong, C.,
590 Chen, S., Jiang, C., Xie, N., Zheng, X., Wang, Y., Song, C., Peters. R.J., & Chen, S. (2019).
591 The genome of the medicinal plant *Andrographis paniculata* provides insight into the
592 biosynthesis of the bioactive diterpenoid neoandrographolide. *The Plant Journal*, *97*, 841-857
- 593 Tamura, K., Dudley, J., Nei, M. & Kumar, S. (2007) MEGA4: Molecular evolutionary genetics
594 analysis (MEGA) software version 4.0. *Molecular Biology and Evolution*, *24*, 1596-1599.
- 595 Trapnell, C., Williams, B.A., Pertea, G., Mortazavi, A., Kwan, G., van Baren, M.J., Salzberg, S.L.,
596 Wold, B.J., & Pachter, L. (2010). Transcript assembly and quantification by RNA-Seq reveals
597 unannotated transcripts and isoform switching during cell differentiation. *Nature*
598 *Biotechnology*, *28*, 511-555.
- 599 Tsuji, K., & Ohnishi, O. (2000). Origin of cultivated Tatar buckwheat *Fagopyrum tataricum*
600 Gaertn. revealed by RAPD analysis. *Genetic Resources and Crop Evolution*, *47*, 431-438.
- 601 Wu, B., Gao, L., Gao, J., Xu, Y., Liu, H., Cao, X., Zhang, B., & Chen, K. (2017). Genome-wide
602 identification, expression patterns, and functional analysis of UDP glycosyltransferase family
603 in peach *Prunus persica* L. Batsch. *Frontiers in Plant Science*, *8*, 389.

- 604 Xie, K.B., Chen, R.D., Li, J.H., Wang, R.S., Chen, D.W., Dou, X.X., & Dai, J.G. (2014). Exploring
605 the catalytic promiscuity of a new glycosyltransferase from *Carthamus tinctorius*. *Organic*
606 *Letter*, 16, 4874-4877.
- 607 Xu, J., Chu, Y., Liao, B., Xiao, S., Yin, Q., Bai, R., Su, H., Dong, L., Li, X., Qian, J., Zhang, J.,
608 Zhang, Y., Zhang, X., Wu, M., Zhang, J., Li, G., Zhang, L., Chang, Z., Zhang, Y., Jia, Z., Liu,
609 Z., Afreh, D., Nahurira, R., Zhang, L., Cheng, R., Zhu, Y., Zhu, G., Rao, W., Zhou, C., Qiao,
610 L., Huang, Z., Cheng, Y.C., & Chen, S. (2017). *Panax ginseng* genome examination for
611 ginsenoside biosynthesis. *GigaScience*, 6, 1-15.
- 612 Yin, Q.G., Shen, G.A., Chang, Z.Z., Tang, Y.H., Gao, H.W., & Pang, Y.Z. (2017). Involvement of
613 three putative glucosyltransferases from the UGT72 family in flavonol glucoside/rhamnoside
614 biosynthesis in *Lotus japonicus* seeds. *Journal of Experimental Botany*, 68, 594-609.
- 615 Zhang, D., Jiang, C., Huang, C., Wen, D., Lu, J., Chen, S., Zhang, T., Shi, Y., Xue, J., Ma, W.,
616 Xiang, L., Sun, W., Chen, S. (2019) The light - induced transcription factor FtMYB116
617 promotes accumulation of rutin in *Fagopyrum tataricum*. *Plant Cell Environment*, 42,
618 1340-1351.
- 619 Zhang, L.J., Li, X.X., Ma, B., Gao, Q., Du, H.L., Han, Y.H., Li, Y., Cao, Y., Qi, M., Zhu, Y., Lu,
620 H., Ma, M., Liu, L., Zhou, J., Nan, C., Qin, Y., Wang, J., Cui, L., Liu, H., Liang, C., Qiao, Z.
621 (2017). The tartary buckwheat genome provides insights into rutin biosynthesis and abiotic
622 stress tolerance. *Molecular Plant*, 10, 1224-1237.
- 623 Zhang, W., Ye, M., Zhan, J., Chen, Y., & Guo, D. (2004). Microbial glycosylation of four free
624 anthraquinones by *Absidia coerulea*. *Biotechnology Letters*, 26, 127-131.
- 625 Zhou, J., Li, C.L., Gao, F., Luo, X.P., Li, Q.Q., Zhao, H.X., Yao, H.P., Chen, H., Wang, A.H., &
626 Wu, Q. (2016). Characterization of three glucosyltransferase genes in Tartary buckwheat and
627 their expression after cold stress. *Journal of Agricultural and Food Chemistry*, 64, 6930-6938.
- 628

629

630 **Figure Captions**

631

632 **Figure 1** Phylogenetic analysis of UGTs in *F. tataricum*

633

634 Amino acid sequences were analyzed using Clustal X2 and the bootstrap consensus tree was
635 constructed using MEGA 4.0 with the neighbor-joining method and 1000 bootstrap replicates. The
636 respective protein names and numbers are listed in Supplementary Data S1. UGTs from *F.*
637 *tataricum* are marked in green and those from *Arabidopsis* in black. The groups are marked in
638 different colors.

639

640 **Figure 2** Hierarchical clustering analysis of transcript levels of UGT genes in different tissues and
641 seed development stages of *F. tataricum*.

642

643 FtUGTs marked green were the candidates for further study. R was the abbreviation of roots; St,
644 stem; L, leaf; F, flower; Sd1-Sd3 means prophase, mid-term, later period of ovary bulge, Sd4-Sd6
645 means prophase, mid-term, later period of grout, and Sd7-Sd9 means prophase, mid-term, later
646 period of mature. The clustering was performed using Heatmap2. The heat map shows relative
647 transcript level of FtUGT genes in various tissues. The color scale (-3 to 3 in green to red color)
648 represents Z-score-normalized gene expression. Dendrograms along the top and left sides of the
649 heat map indicate the hierarchical clustering of tissues and genes.

650

651 **Figure 3** Identification of the enzymatic product of recombinant FtUGT73BE5 protein by HPLC
652 and UPLC/MS/MS

653

654 Diagram A and D represent HPLC chromatographs of the enzymatic products containing quercetin
655 (Q), quercetin 3-*O*-glucoside (QG) and emodin (E) with recombinant FtUGT73EB5, respectively.
656 Diagrams B, C and E are the tandem mass spectrum of the enzymatic products of recombinant
657 FtUGT73EB5 protein with Q, QG and E determined by UPLC/MS/MS, respectively. G, Glucoside.
658

659 **Figure 4** The characteristics of FtUGT73BE5 proteins

660
661 (A) Kinetic parameters of the recombinant FtUGT73BE5 and FtUGT75R2 proteins with flavonol
662 aglycones or emodin as acceptor substrate and UDP-glucose as donor substrate. Values represent
663 the means \pm SD from triplicate enzymatic assays. (B) the proposal glucosylation of rutin and
664 emodin 6-*O*-glucoside. (C) Representative binding domain (left panel) and the overall view of the
665 structural model of FtUGT73BE5 docking with UDP-glucose and quercetin 3-*O*-glucose. The
666 amino acids in the form of ligands with UDP-glucose donor and acceptor are highlighted in black.
667 UPG was abbreviated from UDP-glucose (blue stick); Q, quercetin; QG, quercetin 3-*O*-glucose
668 (green stick). KG, kaempferol 3-*O*-glucose; E, emodin.

669

670 **Figure 5** Identification of FtUGT73BE5 *in vivo*

671

672 (A) Transgenic hairy roots of *F. tataricum* detected under bright field and GFP florescence. (B)
673 Transcript levels of FtUGT73BE5 in control (CK) and transgenic hairy roots (overexpression)
674 detected by qRT-PCR. (C) Flavonol glucosides content in overexpressing hairy roots; left, the
675 content of quercetin 3-*O*-glucoside (QG); right, the content of rutin. (D) Representative MS
676 chromatographs of the metabolic extracts from transgenic line (first panel) and empty vector (CK,
677 second panel), the third and last panel shows the MS chromatographs of enzymatic product and
678 emodin (E). (E) Contents of emodin 6-*O*-glucoside (E 6-*O*-G) in vector control (CK) and transgenic
679 hairy roots supplied with emodin.

680

681 **Figure 6** Expression profiles of FtUGTs and its relationship with hormones

682

683 (A) Relative expression of *FtUGT73BE5* and *FtUGT75R2*, and rutin contents in various tissues of *F.*
684 *tataricum*. (B) The relative expression of *FtUGT73BE5* and *FtUGT75R2* in seedlings after treated
685 by ABA(4h, 14h, 24h) and MeJA (4h, 14h, 24h). (C) The contents of rutin, quercetin and quercetin
686 3-*O*-glucoside in seedlings after treated by ABA (4h, 14h, 24h) and MeJA (4h, 14h, 24h).

687

688 SUPPLEMENTARY DATA

689

690 **Supplementary Table S1** Candidate FtUGTs by phylogenetic and transcriptomics analysis

691

692 The bold UGTs were cloned successfully.

693

694 **Supplementary Table S2** The enzymatic activity of five recombinant FtUGT proteins toward
695 flavonoids and emodin with UDP-glucose

696

697 4-coumaric acid (4-C), naringenin (Na), kaempferol (Ka), quercetin (Q), quercetin 3-*O*-glucoside
698 (QG), quercitrin (QG'), catechin (C), flavone (Fl, CAS number, 525-82-6), apigenin(A), luteolin
699 (L) and emodin (E). A dash (-) indicates the assay was not done.

700

701 **Supplementary Table S3** The information of ion fragment of flavonoids and emodin for QqQ
702 quantification

703

704 **Supplementary Data S1** Transcripts and names of FtUGTs

705

706 **Supplementary Data S2** Primer sequences used in this study

707

708 **Supplementary Figure S1** Key genes involved in rutin and emodin glucoside schematic
709 biosynthetic pathway of *F. tataricum*

710 (A) the general biosynthetic pathway of rutin. CHS, chalcone synthase; CHI, chalcone isomerase;
711 F3H, flavanone 3-hydroxylase; F3'H, flavonoid 3'-hydroxylase; FLS, flavonol synthase; UGT,
712 UDP glycosyltransferase. (B) the general biosynthetic pathway of emodin. PKS, polyketone
713 synthase; CYP450, cytochrome P450; E6G, emodin 6-O-glucose; Gly, glucose. Solid lines mean
714 one step; dashed lines mean multiple steps.

715

716 **Supplementary Figure S2** Intron distribution of 106 UGT genes in *F.tataricum*

717

718 Yellow column representative CDS (coding sequence); purple column, UTR (untranslated coding
719 regions); line, intron; red column, 5'UTR; green column, starting codon; orange column, stop codon;
720 grey column, 3'UTR.

721

722 **Supplementary Figure S3** Deduced chromosomal positions of FtUGT genes

723

724 **Supplementary Figure S4** Sequence analysis and protein expression of candidate FtUGTs

725 (A) Represents of Molecular phylogenetic tree of identified FtUGTs. (B) PSPG boxes alignment of
726 cloned FtUGTs. (C) The SDS-PAGE gel map of FtUGTs possessing activity to the tested substrates.
727 Multiple sequences were aligned by Clustal X2 and used for tree constructions with the maximum
728 likelihood method using MEGA4. Bootstrap values from 1000 replicates are shown on branches
729 (values > 50% are shown). Bar represents 0.5 amino acid substitutions per site. GenBank accessions
730 are as follows: At3G7GT, NP_181217.1[*Arabidopsis thaliana*]; At5GT, NP_193146.1[*Arabidopsis*

731 *thaliana*]; At7G1, NP_561955.1[*Arabidopsis thaliana*]; Cm1,2Rha1, Q8GVE3.2[*Citrus maxima*];
 732 Ct3GT, 3WC4_A[*Clitoria Ternatea*]; GeIF7GT, BAC78438.1[*Glycyrrhiza echinata*]; Ih3GT,
 733 BAD83701.1[*Iris x hollandica*]; Ip3GGT, Q53UH5.1[*Ipomoea purpurea*]; PfA5GT,
 734 Q9ZR27.1[*Perilla frutescens*]; VhA5GT, Q9ZR25.1[*Glandularia x hybrida*]; VmF3GT,
 735 BAA36972.1[*Vigna mungo*]; Vv3GT, P51094.2[*Vitis vinifera*]; Zm3GT, P16165.1[*Zea mays*];
 736 Sb7GT, BAA83484.1[*Scutellaria baicalensis*]; ThA5GT, BAC54093.1[*Torenia hybrid cultivar*];
 737 PhA3G6"RT, CAA50376.1[*Petunia x hybrida*]; PhA5GT, BAA89009.1[*Petunia x hybrida*]; Fi3GT,
 738 AAD21086.1[*Forsythia x intermedia*]; Hv3GT, P14726.1[*Hordeum vulgare*]; Cm7G2"RT,
 739 ACX70154.1[*Citrus maxima*]; IpA3G2"GT, Q53UH5.1[*Ipomoea purpurea*]; At7RT,
 740 NP_563756.1[*Arabidopsis thaliana*]; At3RT, NP_564357.1[*Arabidopsis thaliana*]; Lb7GlcT,
 741 BAG80536.1[*Lycium barbarum*]; Am7GT, BAG16513.1[*Antirrhinum majus*]; CtUGT73AE1,
 742 AJT58578.1[*Carthamus tinctorius*]. FtUFGT2, AOS85163.1[*Fagopyrum tataricum*];
 743 FtUGT714B1,AOS85162.1[*Fagopyrum tataricum*]; FtUGT714C1, AOS85164.1[*Fagopyrum*
 744 *tataricum*]; FtUGT71AG1, APY21160.1[*Fagopyrum tataricum*]; FtUGT71U4,
 745 APY21161.1[*Fagopyrum tataricum*]; FeUGT708C1, BAP90360.1[*Fagopyrum esculentum*];
 746 FeUGT708C2,BAP90361.1[*Fagopyrum esculentum*]; FeCGTv, BAP90374.1[*Fagopyrum*
 747 *esculentum*];

748

749 **Supplementary Figure S5** MS detection of Products catalyzed by rUGT73BE5 with others
 750 substrates

751

752 **Supplementary Figure S6** MS detection of Products catalyzed by rUGT75R2 with others
 753 substrates

754

755 **Supplementary Figure S7** *In vitro* activity identification of FtUGT73BE5 related to emodin

756

757 Glucosylation site verification of products by HPLC (A) and MS (B); panels of HPLC (A) are
758 FtUGT73BE5 with E (emodin), E (authentic emodin), E 1-*O*-G (authentic emodin 1-*O*-glucoside),
759 and E 8-*O*-G (authentic emodin 8-*O*-glucoside) from top to bottom; MS chromatograms of E 1-*O*-G
760 (first panel), E 8-*O*-G (second panel), product (third panel) and E (last panel) are shown in B.

761

762 **Supplementary Figure S8** The characterization of rUGT73BE5

763

764 (A) Represents optimum temperature for rUGT73BE5 for quercetin 3-*O*-glucoside and emodin; the
765 assay mix (100 μ L) contained 2.5 μ g purified protein, 2 mM UDP-glucose, 10 mM DTT, 100 μ M
766 quercetin or emodin and 50 mM Tris-HCl (pH 7.0) for 30 min. (B) shows optimum pH value for
767 rUGT73BE5, the reaction was carried out at 37 °C for 30 min. (C) The reaction rates of
768 rUGT73BE5 toward 10 substrates, the reaction was carried out at 37 °C for 30 min with 50 mM
769 Tris-HCl (pH 7.0). naringenin (Na), kaempferol (Ka), quercetin (Q), quercetin 3-*O*-glucoside (QG),
770 quercitrin (QG'), catechin (C), flavone (Fl, CAS number, 525-82-6), apigenin(A), luteolin (L) and
771 emodin (E).

772

773 **Supplementary Figure S9** The inhibition of rutin biosynthesis in *FtUGT73BE5*-RNAi hairy roots

774

775 (A) Transcript levels of *FtUGT73BE5* in control (CK) and RNAi hairy roots detected by qRT-PCR.

776 B&C represent contents of quercetin 3-*O*-glucoside and rutin in transgenic lines, respectively.

777 **Credit Author Statement**

778

779 QY, XH, WS and SC: Supervision, conceived and designed the study. QY, XH, ZH, and CX: Investigation, performed
780 the experiments and analyzed the data. QY: Writing-Original draft preparation, Writing- Reviewing and Editing.
781 QC, YS, GD and CS: Writing-Reviewing and Editing. QC and GD: Resources, provided the seeds of tartary
782 buckwheat. HG and TZ: Data curation, Formal analysis, analyzed the UGTs information from transcriptome and
783 genome. All authors read and approved the manuscript.

784

- 785 1. Temporal and spatial transcripts of 106 FtUGTs were analyzed in genome level.
786
- 787 2. FtUGT73BE5 was identified to dominate the first step of rutin glycosylation.
788
- 789 3. FtUGT73BE5 was demonstrated to catalyze emodin to form emodin 6-*O*-glucoside.
790
- 791 4. MeJA up-regulates transcript of *FtUGT73BE5*; it was related to anti-adversity.
792
- 793
- 794